JNPS 10 (2): 1-7 (2024)
ISSN: 2392-473X(Print), 2738-9537 (Online)

Research Article *©Nepal Physical Society*
doi.org/10.3126/jnphyssoc.v10i2.79467

Geomagnetic Fields and Total Electron Content Variations at Eagle Station During Solar Storms of Solar Cycle 24

Ashutosh Giri[1], Ismal Bahadur Pudasaini[2], Suruchi Shahi Thakuri[2], Uluma Edward[4], Bigyan Mainali[1], Kiran Pudasainee[3], Chali Idosa Uga[1], Rajendra Adhikari[5] and Binod Adhikari[6] *

[1]Department of Space Science, University of Alabama in Huntsville, Alabama, USA.
[2]Department of Physics St. Xavier's College, Kathmandu, Nepal.
[3]Department of Physics, Tri-Chandra Multiple College, Tribhuvan University, Nepal.
[4]Department of Physics, Masinde Muliro University of Science & Technology, Kakamega, Kenya.
[5]Department of Physics, Amrit Campus, Tribhuvan University, Nepal.
[6]Department of Physics, Patan Multiple College, Tribhuvan University, Nepal.
**Corresponding Author: Binod Adhikari*
Email: binod.adhi@gmail.com

Submitted: September 25, 2024; **Revised:** May 24, 2025; **Accepted:** June 1, 2025

Abstract:

In this work, we analyzed variations in the Earth's magnetic field components (D, H, and Z), interplanetary magnetic field (IMF-Bz), interplanetary electric field (IEF-Ey), and GPS-derived total electron content (TEC) during three solar storms observed over Eagle Station (64.7860°N, 141.1999°W) in Canada during Solar Cycle 24. The selected events include a moderate storm (25–27 October, 2011), an intense storm (15–19 March, 2015), and a weak storm (6–10 May, 2018). The results indicate that solar storms caused notable disturbances in all components of the geomagnetic field, with the D, H, and Z components showing marked decreases during storm periods. These disturbances were accompanied by a corresponding increase in TEC. Additionally, the degree of geomagnetic variation was closely linked to the intensity of geomgantic storms. These disturbances are likely driven by enhanced magnetospheric convection and increased particle precipitation into the high-latitude ionosphere, primarily resulting from prolonged southward IMF-Bz orientations and strengthened solar wind–magnetosphere coupling during geomagnetic storm conditions.

Keywords: GEOMAGNETIC STORM; TOTAL ELECTRON CONTENT (TEC); INTERPLANETARY MAGNETIC FIELD (IMF), CORONAL MASS EJECTION (CME), SOLAR WIND PARAMETERS

1. Introduction

Extreme space weather conditions like geomagnetic storms have a huge impact on climate and other components of the ionosphere such as Total Electron Content (TEC). Geomagnetic storms result from the interaction of the energetic solar wind and the Earth's magnetic field, affecting the southward interplanetary magnetic

field z-component (IMF-B_z) [1]. The disturbance of the Earth's magnetic field due to geomagnetic storms usually changes the ionospheric TEC variation [2]. TEC variation refers to the fluctuation in the Total Electron Content, which represents the integral of electron density along a path typically perpendicular to the Earth's surface, reaching upward to a defined altitude within the ionosphere. These changes reflect dynamic alterations in ionospheric electron density, influenced by factors like solar activity, geomagnetic storms, and other atmospheric phenomena. Geomagnetic storms can either be positive ionospheric storms or negative ionospheric storms [2]. [3] defined a positive ionospheric storm as the increase in electron density during the storm while a negative ionospheric storm was defined as the depletion of electron density during the storm.

When solar material with magnetic properties encounters Earth's magnetic field, it has the potential to trigger geomagnetic storms or space weather. Coronal mass ejections (CMEs) from the Sun's corona are ejected radially outwards due to the effect of the rotation of the Sun and the radial outward motion of the plasma [4]. Interplanetary Coronal Mass Ejections (ICMEs) contain electrons, ions, and other solar particles having large amounts of energy [5], which are propagated hemispherically [6]. The amount of energy transferred to the magnetosphere largely depends on the north-south components of the IMF-B_z. The amount of energy transferred increases when the IMF has a large magnitude ($\geq$ 10 nT) and a large southward component [4]. The northward turning of the IMF leads to reduced energy transfer [7]. Great geomagnetic storms are not caused by the solar wind but are caused by increased southward turning of the IMF-B_z [8]. Scientific analysis of geomagnetic storms is very important in understanding the surrounding space weather environment [9]. This enables the assessment and mitigation of space weather-related hazards, satellite communication and navigation, and geophysical surveys [10].

[1] studied the variation of solar wind parameters and TEC from Indian, Australian, Brazilian and South African sectors during intense geomagnetic storms of 2015. They analyzed VTEC data from 12 GPS stations, solar wind parameters (Vsw, Nsw, Psw) and Geomagnetic indices (AE and SYM\H). Their results showed the impact of geomagnetic storms was felt in all the studied regions except the Indian region. The modification of ionospheric dynamics at the equatorial and low latitudes was attributed to the effect of prompt penetration of the magnetospheric electric field during the main phase of the storm when the Dst index fluctuated sharply. [11] studied the variation of ionospheric TEC during geomagnetic storms in the 24th solar cycle. They used GPS-TEC data from Bangalore which was a low-latitude station in India. The obtained results showed the geomagnetic storm influencing the F layer. [4] studied the analysis of cosmic rays, solar wind energies, components of the Earth's magnetic field, and ionospheric TEC during a solar superstorm of 18th -22nd November 2003. A comprehensive study was conducted for different parameters such as solar wind speed, density, plasma temperature, plasma pressure, auroral electrojet, SYM\H, energy transfer, components of Earth's magnetic field, TEC and cosmic rays received by the Earth during the storm. It was observed that the

solar storm of November 2003 had a SYM\H value of -472 nT. During the main phase of the storm, the velocity of the solar wind reached approximately 500km/s and plasma pressure accumulated to around 20 nPa. The decrease in the rate of cosmic rays received by the Earth during the main phase of the storm indicated the existence of the inverse relation between the strength of the solar storm and the amount of cosmic ray fluxes received by the Earth.

In this paper, we have studied the selected events which include a moderate storm (25th – 27th October 2011), an intense storm (15th – 19th March 2015), and a weak storm (6th – 10th May 2018) and analyzed the variations in the Earth's magnetic field components (D, H, and Z), interplanetary magnetic field (IMF-Bz), interplanetary electric field (IEF-Ey), and GPS-derived TEC over Eagle Station (64.7860°N, 141.1999°W). Section 2 describes the dataset and method used in this study. Section 3 presents the results along with a detailed discussion, while Section 4 provides a concise conclusion of the research findings.

2. Dataset and Method

In this study, geomagnetic field components and geomagnetic indices for three selected storms during Solar Cycle 24 were obtained from the OMNI database (https://omniweb.gsfc.nasa.gov/form). GPS-derived TEC data for the Eagle GNSS receiver station in Canada, corresponding to the storm periods, were sourced from the University NAVSTAR Consortium (UNAVCO) dual-frequency devices (http://unavco.org/data/gps-gnssdata/). The GPS-TEC data in the GNSS receiver is saved in the zipped Receiver Independent Exchange (RINEX) Format. The data was unzipped using WinRAR and processed using Gopi software to obtain a text (.cmn output) file which is a more simplified ten-column daily file of ionospheric observables separated by a tab: Jdatet, Time, PRN, Az, Ele, Lat, Lon, Stec and VTEC and a mean TEC output (Std) file in the directory of data files. The. cmn output files for the selected storm days were considered for further analysis [12].

3. Results and Discussions

In this section, we discuss the variations in components of geomagnetic fields and TEC over Eagle station of Canada during selected events.

3.1. Event 1: 25th – 27th October 2011

A long-duration solar flare with an X-ray M1.3 classification took place on October 22, 2011. Its onset was at 10:00 UT, it reached maximum intensity at 11:10 UT and ended at 13:09 UT. This solar flare was linked to a CME that had a mainly northward direction and an estimated plane-of-sky speed of 600 kilometres per second, as observed by STEREO-A COR2. Imaging from LASCO C2 and C3 detected a partial CME halo with a maximum plane-of-sky speed of 1000 kilometres per second at its northernmost edge [SWPC PRF 1886, 2011]. A weak Hα flare from Region 1314 (N28W77) was also noted on October 22. It began before 12:32 UT, peaked around 12:52 UT, and lasted until at least 13:28 UT. The X-ray M1.3 solar flare observed on 22 October led to a proton event with energies exceeding 10 mega electron volts.

This event was detected on 23 October at the GOES satellite position. The proton event, classified as an S1-Minor solar radiation storm according to NOAA Space Weather scale (http://www.swpc.noaa.gov/NOAAscales/), commenced at 15:00 UT, reached its peak at 13 proton flux units (1 proton flux unit = 1 particle/s/sr/cm^2) at 15:35 UT, and concluded at 16:05 UT [SWPC PRF 1886, 2011]. Besides solar flares, various types of ionospheric effects

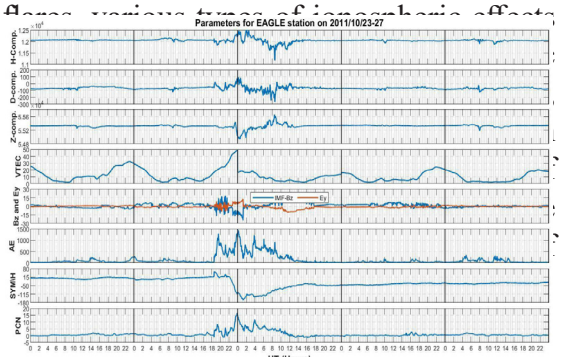

Figure 1: Space weather and geomagnetic indices during the storm of 23-27th October 2011. From the top panel to the bottom panel, the top panel – H-component; the second panel –D-component; third panel-Z-component; the fourth panel – VTEC; the fifth panel- Bz and Ey; the sixth panel- AE (nT); the seventh panel- SYM\H and eighth panel- PCN.

Figure 1 shows the H, D, and Z geomagnetic field components alongside Bz, Ey, AE, SYM\H, and PCN indices, all remaining relatively stable with minimal fluctuations until 18:00 UT on October 24, 2011. The onset of a moderate geomagnetic storm is observed from that point, lasting until approximately 14:00 UT on October 25, 2011. The effect of a moderate geomagnetic storm in H and D components has shown a similar trend to the SYM\H and IMF-B_z. However, the Z component followed the rather opposite trend of SYM\H and IMF-B_z. The VTEC has shown an increasing trend during the event with a drop after the peak value. The increase in VTEC during the event was caused by induced disturbance through the geomagnetic storm. Upon entering the Earth's magnetic field line, solar energetic particles from CME generate an electric current in the polar region. This current causes disruptions in the magnetosphere and ionosphere, leading to an increase in VTEC during these disturbances.

3.2 Event 2: 15th – 19th March 2015

The intense geomagnetic storm on March 17, 2015, was caused by two interacting Coronal Mass Ejections (CMEs) on March 15. The first CME (CME1) occurred on March 14, travelling at a speed of approximately 350 km s−1 and likely associated with a C2.6 flare from the same active region (S21◦W20◦) that peaked around 11:55 UT on March 14. The second CME (CME2) reached a maximum speed of about 1100 km s^−1 and was associated with a prolonged C9.1 solar flare from AR 12297 (S22◦W25◦) that peaked at 02:13 UT on March 15. Initial observations suggested that CME1 was mainly moving southward while CME2 had a significant component heading west. Despite the relatively weak associated flares, the Earth encountered the side of the CME, contributing to the intensity of the geomagnetic storm. This event resembles the development of the super solar storm that impacted STEREO-A on July 23, 2012. A shock hit the Wind at 04:01 UT on March 17, leading to the sudden onset of the geomagnetic storm [5].

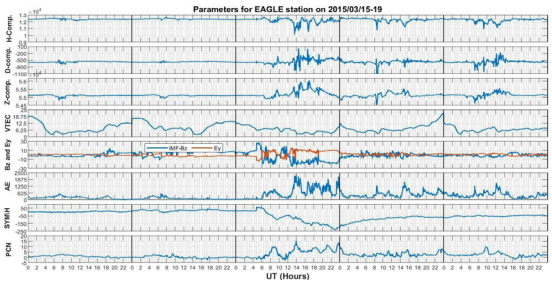

Figure 2: Space weather and geomagnetic indices during the storm of 15-19th March 2015. From the top panel to the bottom panel, the top panel – H-component; the second panel –D-component; third panel-Z-component; the fourth panel – VTEC; the fifth panel- Bz and Ey; the sixth panel- AE (nT); the seventh panel- SYM\H and eighth panel- PCN.

Figure 2 illustrates the H, D, and Z geomagnetic field components, along with Bz, Ey, AE, SYM\H, and PCN indices, all remaining stable with minimal fluctuations until 04:00 UT on March 17, 2017. The intense geomagnetic storm then occurred, lasting until approximately 15:00 UT on March 19, 2017. The effect of an intense geomagnetic storm in H and D components has shown a similar trend to the SYM\H and IMF-B_z. However, the Z components of Earth's magnetic field increased with IEF-E_Y, AE, and PCN indices. The vertical total electron content on the other hand decreased during this intense storm (March 17, 2015). But on 22 UT(Hours) March 18, 2015, the VTEC showed an incremental trend.

3.3 Event 3: 6th – 10th May 2018

A G1 (Minor) geomagnetic storm watch was issued for May 6 and 7, 2018, in response to the expected impact of a negative polarity coronal hole high-speed stream (CH HSS). These high-speed solar wind streams, originating from coronal holes on the Sun, can interact with Earth's magnetosphere, leading to geomagnetic disturbances. Similar to Figure 1 and 2, Figure 3 depicts various space weather and geomagnetic indices recorded at the EAGLE station on 6-10 May, 2018. The magnetic field components, H, and Z show fluctuations from the maximum of nT, and nT to the minimum of nT and nT over time. But the D- component has risen to the negative value of -400 nT from the positive value of 100 nT. The figure shows significant spikes in the AE index multiple times with a maximum value of 1200 nT and a minimum of 0 nT, indicating periods of

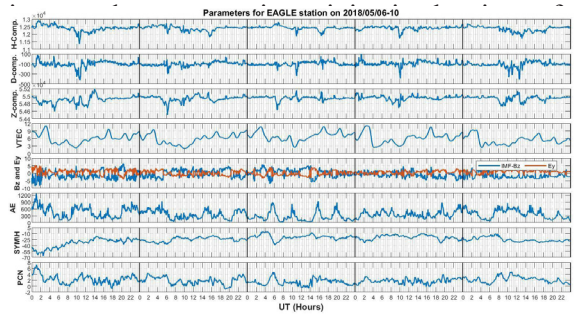

Figure 3: Space weather and geomagnetic indices during the storm of 06-10th May 2018. From the top panel to the bottom panel, the top panel – H-component; the second panel –D-component; third panel-Z-component; the fourth panel – VTEC; the fifth panel- Bz and Ey; the sixth panel- AE (nT); the seventh panel- SYM\H and eighth panel- PCN.

Overall, the results presented in Figures 1, 2, and 3 confirm that variations in the geomagnetic field components (D, H, Z), IMF-Bz, IEF-Ey, and TEC are closely linked to the intensity of geomagnetic storms. Stronger storms led to more pronounced decreases in magnetic field components and significant TEC enhancements. These findings are consistent with earlier studies [4, 13, 14], which attribute such changes to processes like ring current intensification, Joule heating, and ionosphere–thermosphere coupling. These interactions

highlight the dynamic nature of storm-time ionospheric and geomagnetic responses and emphasize the role of solar wind-magnetosphere coupling during disturbed conditions.

4.Conclusion:

In this study, we explored the influence of geomagnetic storms on ionospheric parameters during three events within Solar Cycle 24 over Eagle Station in Canada. Geomagnetic storms, triggered by the interaction of solar wind and the Earth's magnetic field, have substantial effects on the ionosphere, particularly on TEC and various components of the geomagnetic field. The following conclusions can be drawn from this work:

- The geomagnetic storm events on 25-27 October, 2011, 15-19 March, 2015, and 6-10 May, 2018, revealed distinct variations in ionospheric parameters. The H, D, and Z components of the Earth's magnetic field showed trends consistent with the SYM\H index and IMF-B_z components during intense storms. However, the Z component increased with IEF-E_Y, AE, and PCN indices. TEC exhibited a decrease during intense storms but showed an increment trend on specific days.
- These results support previous studies showing that geomagnetic storms affect both the Earth's magnetic field and ionospheric conditions. The findings help improve our understanding of how solar activity influences the upper atmosphere.
- The observed disturbances can be attributed to enhanced magnetospheric convection and increased particle precipitation, driven by sustained southward IMF-Bz and intensified solar wind–magnetosphere coupling during geomagnetic storm conditions.

In summary, our research underscores the importance of studying ionospheric parameters during geomagnetic. The variations observed in the Eagle Station region during selected events of solar cycle 24 provide valuable insights into the complex interactions between solar wind, magnetic fields, and the ionosphere, contributing to the broader understanding of space weather phenomena.

Acknowledgments

The author would like to acknowledge the space weather data archieve of the High-Resolution OMNI (HRO) of NASA, (https://omniweb.gsfc.nasa.gov/). UNAVCO for the data of TEC obtained from GPS satellites in RINEX format. Gopi Seemala interface (https://seemala.blogspot.com/) to process RINEX into ASCII files.

Conflict of Interest

There is no conflict of interests or competing interests.

Funding: Not applicable.

Reference:

[1] R. K. Mishra, B. Adhikari, N. P. Chapagain, R. Baral, P. K. Das, V. Klausner, and M. Sharma, “Variation of solar wind parameters and total electron content from Indian, Australian, Brazilian and

South African sectors during intense geomagnetic storms," *ESSOAR*, 2020, doi: 10.1002/essoar.10503097.1.

[2] K. Davis, *Ionospheric Radio*, London: Peter Peregrinus, 1990

[3] P. R. Fagundes, F. A. Cardoso, B. G. Fejer, K. Venkatesh, B. A. G. Ribeiro, and V. G. Pillat, "Positive and negative GPS-TEC ionospheric storm effects during extreme space weather event of March 2015 over Brazilian sector," *J. Geophys. Res. Space Phys.*, vol. 121, pp. 5613–5625, 2016, doi: 10.1002/2015JA022214.

[4] B. Adhikari, B. Kaphle, N. Adhikari, S. Limbu, A. Sunar, R. M. Mishra, and S. Adhikari, "The analysis of cosmic ray, solar wind energies, components of the Earth's magnetic field and ionospheric TEC during solar super storm of 18th -22nd November 2003," *SN Appl. Sci.*, vol. 1, p. 143, 2019.

[5] N. Gopalswamy, B. Tsunami, and Y. Yan, "Short-term variability of the Sun-Earth system: An overview of progress made during the CAWSES-II period," *Prog. Earth Planet. Sci.*, vol. 2, p. 13, 2015.

[6] W. B. Manchester, T. I. Gombosi, D. L. De Zeeuw, V. Sokolov, I. Roussev, and K. G. Powell, "Coronal mass ejection shock and sheath structures relevant to particle acceleration," *Astrophys. J.*, vol. 622, pp. 1225–1239, 2005.

[7] S. C. Dubey and A. P. Mishra, "Solar activity and large geomagnetic disturbances," *Curr. Sci. Assoc.*, vol. 77, pp. 293–296, 1999.

[8] B. T. Tsurutani, W. D. Gonzalez, and F. Wang, "Geophys. Res. Lett.*, vol. 19, p. 73, 1992.

[9] Y. Kamide and N. Balan, "The importance of ground magnetic data in specifying the state of the magnetosphere-ionosphere coupling: a historical account," *Geosci. Lett.*, 2015.

[10] I. A. Daglis, *Effects of Space Weather on Technology Infrastructure*, Dordrecht: Kluwer Academic, 2004.

[11] S. Kundu, S. Sasmal, S. Chakraborti, and S. Chakrabarti, "The study of ionospheric total electron content (TEC) variation during a geomagnetic storm in 24th solar cycle," in *URSI RCRS 2020*, IIT (BHU), Varanasi, India, Feb. 2020.

[12] G. Seemala and C. Valadare, "Statistics of total electron content depletions observed over the South American continent for the year 2008," *Radio Sci.*, vol. 46, 2011.

[13] C. Nayak, L.-C. Tsai, S.-Y. Su, I. A. Galkin, A. T. K. Tan, E. Nofri, and P. Jamjareegulgarn, "Peculiar features of the low-latitude and mid-latitude ionospheric response to St. Patrick's day geomagnetic storm of 17th March 2015," *J. Geophys. Res. Space Phys.*, vol. 121, pp. 7941–7960, 2016, doi: 10.1002/2016ja022489.

[14] M. Mendillo, "Storms in the ionosphere: Patterns and processes for total electron content," *Rev. Geophys.*, vol. 44, RG4001, 2006, doi: 10.1029/2005RG000193.